PHILOSOPHICAL MAGAZINE A, 1997, VOL. 75, NO. 4, 1117–1127

Slip energy barriers in aluminium and implications for ductile–brittle behaviour

By YUEMIN SUN†§ and EFTHIMIOS KAXIRAS†‡

†Division of Applied Sciences, Harvard University, Cambridge, Massachusetts 02138, USA

‡Department of Physics, Harvard University, Cambridge, Massachusetts 02138, USA

[*Received 30 April 1996 and accepted 27 August 1996*]

ABSTRACT

We consider the ductile–brittle behaviour of aluminium in the framework of the Peierls-model analysis of dislocation emission from a crack tip. To this end, we perform first-principles quantum mechanical calculations for the unstable stacking energy γ_{us} of aluminium along the Shockley partial slip route. Our calculations are based on density functional theory and the local density approximation and include full atomic and volume relaxation. We find that, in aluminium, $\gamma_{us} = 0{\cdot}224\,\mathrm{J\,m^{-2}}$. Within the Peierls-model analysis, this value would predict a brittle solid which poses an interesting problem since aluminium is typically considered to be ductile. The resolution may be given by one of three possibilities: firstly, aluminium is indeed brittle at zero temperature and becomes ductile at a finite temperature owing to motion of pre-existing dislocations which relax the stress concentration at the crack tip; secondly dislocation emission at the crack tip is itself a thermally activated process; thirdly aluminium is actually ductile at all temperatures and the theoretical model employed needs to be significantly improved in order to resolve the apparent contradiction.

§ 1. INTRODUCTION

Understanding the ductile–brittle (D–B) response of materials is both scientifically challenging and technologically important. The D–B response of most metals is usually established by experimental methods. A theoretical framework that can describe quantitatively D–B behaviour has been pursued for over two decades, beginning with the seminal work of Rice and Thomson (1974). When dealing with complicated high-performance materials, such as intermetallic compounds and silicides, the ability to predict the D–B behaviour from theoretical considerations becomes even more important, since experimental measurements are not available or are difficult and time consuming. So far, approximate estimates are available for certain systems, based on atomistic simulations that employ simple interatomic potentials (Cheung 1990, Sun, Rice and Truskinovsky 1991, Beltz and Rice 1992, Sun, Beltz and Rice 1993). Using a Peierls (1940) type of analysis, Rice and co-workers (Rice 1992, Rice, Beltz and Sun 1992, Sun *et al.* 1993, Rice and Beltz 1994, Sun and Beltz 1995) have recently developed simple criteria to characterize the D–B behaviour. These criteria use few key parameters related to the properties of

§ Present address: Pizzano & Co. Inc., 92 Montvale Avenue, Suite 3750, Stoneham, Massachusetts 02180, USA.

the solid, namely the unstable stacking energy, the surface energy, the shear modulus and the Burgers vector. Zhou, Carlsson and Thomson (1993, 1994) have also developed similar criteria that involve these parameters, using atomistic studies of model systems. Of these parameters, the one that is not accessible experimentally is the unstable stacking energy γ_{us}, identified by Rice (1992) to be the quantity that controls the emission of straight dislocations from the crack tip under shear loading. The value of γ_{us} is the lowest energy barrier that needs to be surmounted when one half of a crystal slides over the other half in going from one ideal configuration to another equivalent configuration (the lowest barrier may actually occur between an ideal and a metastable configuration, corresponding to nucleation of partial dislocations). The importance of this quantity within the Peierls model makes it desirable to obtain as accurate estimates as possible for γ_{us} in various materials. Kaxiras and Duesbery (1993) have used first-principle quantum mechanical calculations in the context of density functional theory (DFT) to obtain the value of the unstable stacking energy for silicon, a prototypical covalent material. Here we perform similar calculations for aluminium, a representative simple metal, and analyse the implications of the results for the D–B behaviour of aluminium. Related work on the theoretical strength of aluminium using first-principles quantum-mechanical calculations has been reported by Paxton, Gumbsch and Methfessel (1991).

The metallic nature of aluminium and the relatively small energy cost for the slip (compared, for example, with silicon) require more attention to computational details. Before embarking on the calculation of γ_{us}, we performed several tests to determine the limitations of our calculations. These tests are described in §2. In §3 our results for γ_{us} are discussed and §4 concludes with some discussion of the implications of our results for the D–B behaviour of aluminium in the context of current theories.

§ 2. First-principles calculations for aluminium

Our first-principles calculations are based on DFT (Hohenberg and Kohn 1964) in the local density approximation (LDA) (Kohn and Sham 1965). We employ the expression for the exchange-and-correlation functional proposed by Perdew and Zunger (1981), and a norm-conserving non-local pseudopotential from Bachelet, Haman and Schlüter (1982) to represent the atomic core and eliminate the core electrons of aluminium. A plane-wave basis is used to expand the wavefunctions of the Kohn–Sham orbitals. Since the physical quantities of interest involve obtaining small energy differences by subtracting large numbers, particular care must be taken to assess the uncertainty in these numbers. There are two sources of errors: the first has to do with computational choices, such as limiting the plane wave basis to sets with kinetic energy up to a maximum value, and approximating integrals over the Brillouin zone (BZ) by sums over finite sets of reciprocal space points (k points); the other source of error has to do with inherent limitations of the formalism that we employ. To minimize the first type of error we variationally expanded the plane wave basis and enlarged the sets of k points used in reciprocal-space integrations to the extent possible. From extensive convergence studies we find that the theoretical results are reasonably well converged with a plane wave cut-off of 12 Ryd (corresponding to 70 plane waves per atom) and a uniform grid of k points corresponding to 16 divisions along each reciprocal-lattice vector (using the scheme of Monkhorst and Pack (1976)). The only exception is the calculation of elastic constants (see below), where a denser grid of k points is necessary, corresponding to 20 divisions along each reciprocal-lattice vector. In order to provide estimates of how much the converged results differ from true physical values, we compare with the values of quantities that can be measured experimentally, specifically the bulk properties and the energy of the intrinsic stacking fault in aluminium. Any residual difference is the error inherent in the calculations due to fundamental limitations of the formalism.

As a first test we have calculated the equilibrium lattice constant and the elastic properties of fcc bulk aluminium. We calculated the energy as a function of lattice constant a at 25 points between $a = 3{\cdot}6$ Å and $a = 6{\cdot}4$ Å. The value of the equilibrium lattice constant is obtained by fitting the computed energies to the universal binding energy relation proposed by Rose, Smith, Guinea and Ferrante (1984), giving $a_0 = 3{\cdot}95$ Å. The experimental lattice constant of aluminium at room temperature is 4·05 Å. In order to compare our theoretical value of the equilibrium lattice constant (which of course is calculated at zero temperature) with the experimental value at room temperature, we use the experimental thermal expansion coefficient $\alpha = 2{\cdot}36 \times 10^{-5}\,\mathrm{K}^{-1}$ (Pearson 1958), to extrapolate between zero and room temperature. This gives a theoretical estimate for the lattice constant at room temperature of 4·02 Å, which is in excellent agreement with experiment. We also calculated the bulk modulus B from the second derivative of the energy with respect to volume, evaluated at the minimum. We obtain $B = 84{\cdot}8$ GPa compared with the experimental result of 76·93 GPa. This difference of 10% is typical of DFT–LDA calculations.

In addition to a_0 and B, we have calculated the elastic constants $C_{11} - C_{12}$ and C_{44}, which enter in the expression of the shear modulus $\mu = (C_{11} - C_{12} + 3C_{44})/5$. The elastic constants were obtained using the stress–strain relations and inducing appropriate distortions of the unit cell. The amount of the distortion was large enough to produce energy diferences that can be calculated accurately, with typical distortions in the range 4–8%. The values of the elastic constants and the shear modulus are sensitive to the lattice constant of the crystal. Accordingly, we have performed the calculation at two different lattice constants: the theoretical value at zero temperature ($a_0 = 3{\cdot}95$ Å), and the experimental value at room temperature ($a_0' = 4{\cdot}05$ Å). The results are given in table 1. The agreement with experiment is poor at the theoretical lattice constant at zero temperature but becomes reasonable at the room-temperature experimental lattice constant. Our results compare favourably with previous calculations performed at the experimental lattice constant a_0' by Mehl and Boyer (1991).

As a final test of the reliability of our approach we have calcualted the intrinsic stacking-fault energy γ_{isf} in aluminium, a value that can be determined experimentally. An additional advantage of performing this calculation is that the technical aspects are identical with the calculation of the unstable stacking energy. Specifically, both the intrinsic stacking-fault energy and the unstable stacking energy can be obtained by considering a slab and shearing it in a periodic fashion by a certain distance. This is illustrated in fig. 1: in 1 (*a*), a top view of the ABCABC stacking of layers in the fcc lattice is displayed with high-symmetry directions identified; in fig. 1 (*b*), a side view is shown, with the slip plane identified. The periodic slab consists of an integer multiple of ABC layers in the [111] direction. In our calcuations we have used slabs with two and three periods (i.e. consisting of six and nine layers respectively in the [111] direction), to check convergence with respect to slab size. For slip $a_0/6^{1/2}$ in the $[12\bar{1}]$ direction, one obtains the intrinsic stacking-fault configuration,

Table 1. Comparison of experimental and theoretical values for the lattice constant a_0, bulk modulus B, elastic constants C_{44} and $C_{11} - C_{12}$, and shear modulus μ, evaluated at the theoretical zero-temperature equilibrium value of the lattice constant (3·95 Å) and the room-temperature experimental value (4·05 Å). The experimental values are taken from Hirth and Lothe (1982). The numbers in parentheses give the percentage difference between theoretical and experimental values.

	a_0 (Å)	B (GPa)	C_{44} (GPa)	$C_{11} - C_{12}$ (GPa)	μ (GPa)
Experiment	4·05	76·9	28·5	46·9	26·5
Present work (at $T = 0$ K)	3·95 (−2%)	84·8 (+10%)	45·5 (+60%)	58·8 (+25%)	39·1 (+48%)
Present work at $a_0' = 4{\cdot}05$ Å			29·7 (+4%)	45·1 (−4%)	26·8 (+1%)
Mehl and Boyer (1991) at $a_0' = 4{\cdot}05$ Å			28·5 (0%)	50·0 (+7%)	27·1 (+2%)

Fig. 1

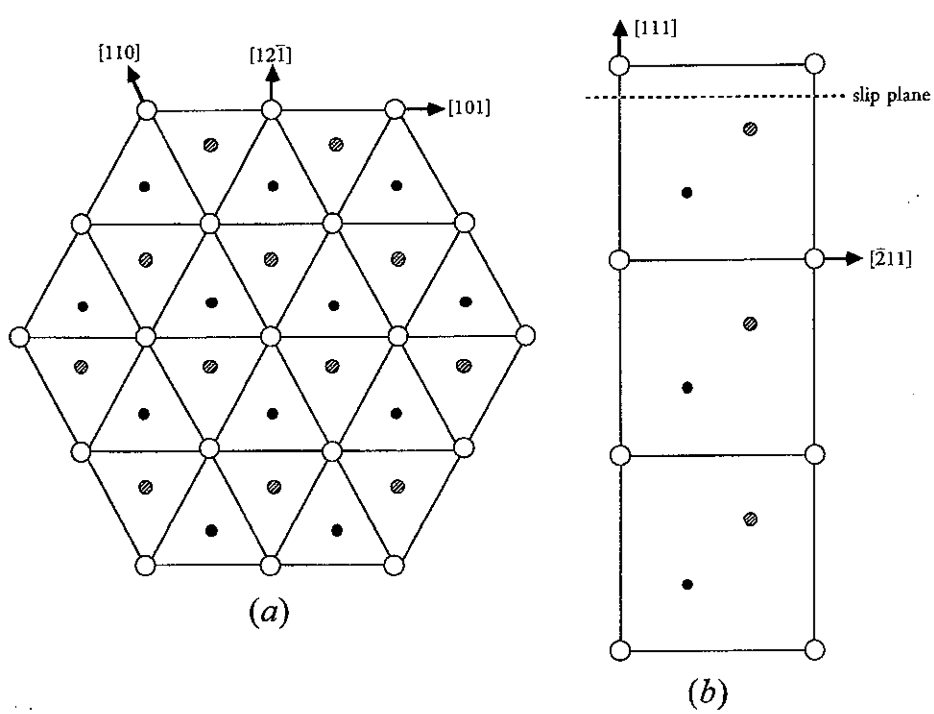

Illustration of the atomic arrangement in fcc aluminium and the slab configuration used in the calculations: (a) top view, (b) side view, indicating the plane on which the crystal is sheared. Atoms in the three layers of stacking along the [111] crystallographic direction are indicted by different symbols.

that is a structure that involves the stacking ABCBCABC, with the stacking fault between the third and fourth layers in the sequence. The unstable stacking energy corresponds to a configuration that is sheared partly from the ideal configuration to the intrinsic stacking-fault configuration by an as yet unspecified amount. For both the intrinsic stacking-fault energy and the unstable stacking energy, we performed the calculations at the theoretically determined lattice constant, which ensures that relaxation according to Hellmann–Feynman forces is realistic and is not due to artificial strains.

Although the results for the six-layer and nine-layer supercells are reasonably close, indicating adequate convergence with respect to supercell size, we have performed an additional test to establish how reliable these numbers are. For this test we used the axial next-nearest-neighbour Ising (ANNNI) model to obtain the energy of the intrinsic stacking fault. Details of this approach can be found in the work of Denteneer and Soler (1991a,b). The advantage of the approach is that very small unit cells can be used to extract the values of the coupling constants, allowing for more extensive convergence tests. The results for γ_{isf} obtained from the ANNNI model and from the supercell calculations differ by at most $0{\cdot}010\,\mathrm{J\,m^{-2}}$ when different k-point sets are used for a plane wave cut-off of 12 Ryd or higher. Our best estimate for the intrinsic stacking-fault value obtained from these calculations is

$$\gamma_{\text{isf}} = 0{\cdot}165 \pm 0{\cdot}015\ \mathrm{J\ m^{-2}}. \tag{1}$$

The error bar was estimated by assuming that the contributions from the size of the plane wave basis, the density of BZ sampling points and the size of the supercell are independent, as experience with similar calculations indicates, with the total error equal to the square root of the sum of squares of the three contributions. Because of the similarity between the intrinsic stacking-fault and the unstable stacking configurations, we expect a similar error for γ_{us}.

The value of γ_{isf} that we obtained is in excellent agreement with the result of Wright, Daw and Fong (1992), $0{\cdot}161\,\mathrm{m^{-2}}$, who used a similar method in their calculations (the plane-wave pseudopotential approach). Our value for γ_{isf} is higher than the result of Denteneer and Soler (1991a), $0{\cdot}126\,\mathrm{J\,m^{-2}}$, which was obtained with a different computational method (the augmented plane-wave approach). Eperimental measurements range from a low of $0{\cdot}110\,\mathrm{J\,m^{-2}}$ to a high of $0{\cdot}280\,\mathrm{J\,m^{-2}}$, with the most recent result of $0{\cdot}150\,\mathrm{J\,m^{-2}}$ obtained by Mills and Sadelmann (1989) (see Wright *et al.* (1992) for additional information). Our calculated value is also in excellent agreement with the experimental value of $0{\cdot}166\,\mathrm{J\,m^{-2}}$ quoted by Hirth and Lothe (1982).

§ 3. Unstable stacking fault

The value of the unstable stacking energy γ_{us} was obtained by shearing half of the infinite crystal over the other half and finding the lowest energy barrier that needs to be overcome in order to bring the crystal from one ideal configuration to another equivalent configuration. The path along which the energy barrier is lowest is in one of the equivalent $\langle 211 \rangle$ crystallographic directions, for instance the $[12\bar{1}]$ direction, shown in fig. 1. Slip along this direction by

$$b_{\text{p}} = \frac{a_0}{6^{1/2}} \tag{2}$$

leads to the intrinsic stacking-fault configuration, which corresponds to a metastable configuration. The unstable stacking energy configuration corresponds to the saddle point along the path from the equilibrium to the metastable configuration, which should occur near, but not necessarily at, the midpoint. To determine the position of the saddle point we calculated the energy for several displacements along the slip path. We refer to these energies as the generalized stacking-fault energy γ_{gsf}. These results are shown in fig. 2. Our calculations indicate that the saddle-point configuration occurs at $0{\cdot}62b_p$. The value of the energy at the saddle-point configuration, before any relaxation is taken into account, is

$$\gamma_{us}^{u} = 0{\cdot}249 \text{ J m}^{-2} \tag{3}$$

When both atomic relaxation and volume relaxation are taken into account, this value drops by $0{\cdot}025 \text{ J m}^{-2}$. Within the Peierls model framework, volume relaxation is meaningful only in the [111] direction. Our estimate of the relaxed unstable stacking energy in aluminium is

$$\gamma_{us}^{r} = 0{\cdot}224 \text{ J m}^{-2} \tag{4}$$

It is useful to express the above results for the unrelaxed and relaxed values of the unstable stacking energy in terms of the dimensionless quantities defined by Sun *et al.* (1993), that provide estimates of the importance of tension–shear coupling. These quantities are defined as

$$q = \frac{\gamma_{us}^{(u)}}{2\gamma_s}, \; p = \frac{\Delta_\theta^*}{L}, \tag{5}$$

Fig. 2

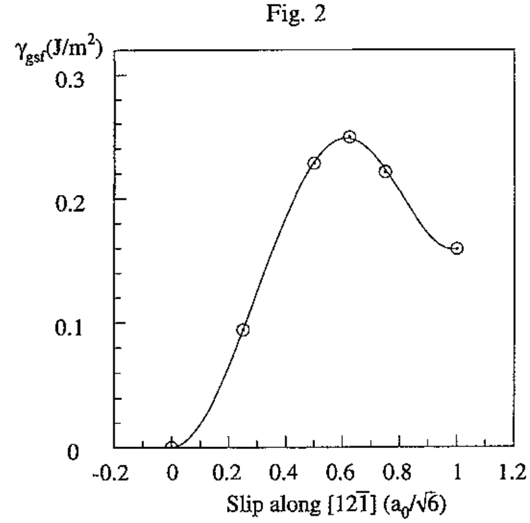

Generalized stacking-fault energy γ_{gsf} as a function of displacement along the slip route in aluminium: (⊙), calculated values; (—), polynomial fit. The maximum in the energy corresponds to the unstable stacking energy γ_{us}, before atomic and volume relaxation. The end point corresponds to the intrinsic stacking-fault energy γ_{isf}. Note that the maximum occurs slightly to the right of the middle.

where γ_s is the energy per unit area of the surface exposed during decohesion, Δ_θ^* is the value of the opening displacement when atomic relaxation is included and corresponding to tensile stress $\sigma = 0$ at the unstable stacking configuration, and L is a phenomenological length scale for tension. The values of the various quantities in the above equations as obtained from the present calculations and from previous work by Sun *et al.* (1993) using the embedded-atom method (EAM), are given in table 2. In this comparison, we have used the value of $\gamma_s = 1{\cdot}10\,\mathrm{J\,m^{-2}}$, from the work of Ferrante and Smith (1979), which was obtained using DFT–LDA calculations. The comparison of the two sets of results in table 2, one from the present first-principles calculations and the other from the empirical EAM calculations, reveals that, while the bare quantities γ_s, $\gamma_{us}^{(u)}$, $\gamma_{us}^{(r)}$ differ by factors of two to three in the two calculations, the dimensionless scaled quantities p, q and L are actually rather close. Apparently, the underestimates of the bare quantities by large factors in the EAM calculations cancel out when the scaled quantities p and q are computed, giving reasonable estimates of the shear to tension coupling.

§ 4. Implications for brittle–ductile behaviour

Significant progress has been made recently in developing criteria for the D–B behaviour by the theoretical analysis of Xu, Argon and Ortiz (1995, 1996, 1997) using the boundary integral method, and the studies by Zhou *et al.* (1993, 1994), using a Green function approach and model atomistic systems. The involved nature of these studies reflects the inherent difficulty in capturing a very complex dynamical phenomenon such as brittleness or ductility, with a few parameters. In the spirit of retaining a simple criterion for the D–B behaviour, it is worthwhile to examine the implications of the present results for aluminium. We shall consider two different contexts. The first is based on the criteria developed by Rice and co-workers (Rice 1992, Rice *et al.* 1992, Sun *et al.* 1993, Rice and Beltz 1994, Sun and Beltz 1995), and the second derives from the atomistic studies of model systems by Zhou *et al.* (1993, 1994).

In the context of the Peierls-type analysis of Rice and co-workers, one can obtain the critical loading G_d for dislocation emission at a crack tip, which depends on the value of γ_{us} and the external loading (assumed here to be mode I), as well as the geometry of the dislocation to be emitted. In the case of aluminium, the relevant dislocation is a Shockley partial, and the parameters entering in the geometry are the

Table 2. The values of the unstable stacking energy $\gamma_{us}^{(u)}$ for the unrelaxed configuration and the unstable stacking energy $\gamma_{us}^{(r)}$ for the relaxed configuration, the surface energy γ_s, the displacement $b/2$ corresponding to the unstable stacking energy along the slip route, the length scale L for tension, and the scaled parameters p and q that determine tension to shear coupling (see text and Sun *et al.* (1993)). The DFT–LDA values are from the present calculation, and the EAM values from the work of Sun *et al.* (1993). The DFT–LDA value of γ_s is from Ferrante and Smith (1979).

	$\gamma_{us}^{(u)}$ ($\mathrm{J\,m^{-2}}$)	$\gamma_{us}^{(r)}$ ($\mathrm{J\,m^{-2}}$)	γ_s ($\mathrm{J\,m^{-2}}$)	$b/2$ (units of $a/6^{1/2}$)	L/b	$p = \Delta\theta^*/L$	$q = \gamma_{us}^{(u)}/2\gamma_s$
DFT–LDA	0·244	0·224	1·10	0·62	0·135	0·111	0·287
EAM	0·092	0·079	0·57	0·50	0·140	0·0854	0·279

tilt angle θ between the slip plane and the extension of the crack, and the angle ϕ between the direction in which the dislocation is emitted and its Burgers vector. These features are illustrated in fig. 3. For the case of tension–shear coupling, the value of G_d (typically given in terms of γ_s, i.e. the ratio $G_d/2\gamma_s$), is obtained by solving numerically a pair of coupled integral equations as described in detail by Sun *et al.* (1993). We have performed such calculations for the slip route described earlier, for several crack geometries denoted by the three vectors $\mathbf{a}_1$, $\mathbf{a}_2$ and $\mathbf{a}_3$, pointing along the crack propagation direction, normal to the crack plane and along the crack line respectively (see fig 3). In these calculations we take the surface energy γ_s to be the same for the (111) and (001) surfaces (which is a reasonable approximation), and we use the experimental values for the elastic constants from Hirth and Lothe (1982), which are very close to the values we obtained at the experimental lattice constant (see table 1).

The results of our calculations are shown in table 3. The geometry labelled A, with $\{\mathbf{a}_1, \mathbf{a}_2, \mathbf{a}_3\} = \{[\bar{1}10], [001], [110]\}$, that is, with a crack on the (001) plane, is interesting in that it produces a ratio $G_d/2\gamma_s > 1$. The easiest slip system for this geometry is on the $(1\bar{1}1)$ plane, along the [121] direction, with corresponding angles $\theta = 54{\cdot}7°$ and $\phi = 60°$. We find that, for this geometry, $G_d/2\gamma_s = 1{\cdot}74$, a value which indicates that dislocation emission is energetically unfavourable compared with crack propagation by cleavage, since according to the Griffith (1920) criterion the critical loading for cleavage is $G_c = 2\gamma_s$. This result then implies that all cracks on (001) planes are brittle and that (001) planes in aluminium are intrinsically cleavable. In light of experimental evidence that suggests aluminium to be ductile, this is a surprising result. We return to this point below.

A different way to link the present results to the intrinsic brittleness or ductility of aluminium is through comparison with recent atomistic calculations on model systems. The work of Zhou *et al.* (1993, 1994) has investigated the conditions for

Fig. 3

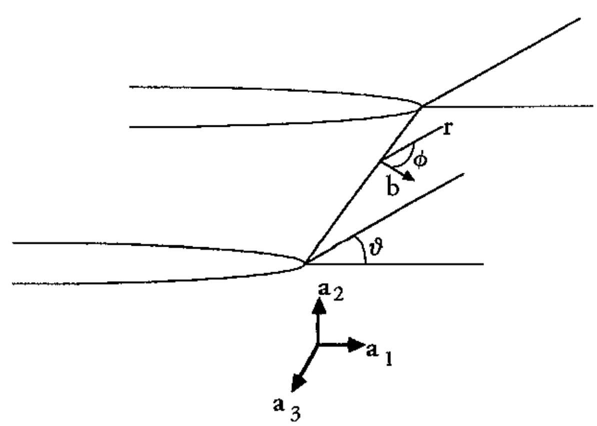

Schematic representation of the geometry for dislocation emission from the crack tip. The vectors $\{\mathbf{a}_1, \mathbf{a}_2, \mathbf{a}_3\}$ are along the extension of the crack, perpendicular to the crack plane and along the crack line respectively. θ is the angle between the crack plane and the inclined plane on which the dislocation with Burgers vector b is emitted, and ϕ is the angle between the emission direction and the Burgers vector.

Table 3. Ratio of the critical loading for dislocation emission G_d to cleavage energy $2\gamma_s$, as obtained from the Peierls model analysis, for various configurations of the slip plane and the emitted dislocation, characterized by the three vectors $\{\mathbf{a}_1, \mathbf{a}_2, \mathbf{a}_3\}$ and the angles (θ, ϕ) (see text and fig. 3). A ratio greater than unity indicates brittle failure, as in configuration A.

Configuration	$\{\mathbf{a}_1, \mathbf{a}_2, \mathbf{a}_3\}$	Slip system	(θ, ϕ)	$G_d/2\gamma_s$
A	$\{[\bar{1}10], [001], [110]\}$	$\frac{1}{6}[121](1\bar{1}1)$	(54·7°, 60°)	1·740
B	$\{[001], [\bar{1}10], [110]\}$	$\frac{1}{6}[\bar{1}12](\bar{1}1\bar{1})$	(35·3°, 0°)	0·968
C	$\{[111], [1\bar{1}0], [11\bar{2}]\}$	$\frac{1}{6}[2\bar{1}\bar{1}](11\bar{1})$	(90°, 30°)	0·730
D	$\{[1\bar{1}2], [\bar{1}11], [110]\}$	$\frac{1}{6}[\bar{1}12](\bar{1}1\bar{1})$	(70·5°, 0°)	0·504

D–B behaviour in a model material, which consisted of a two-dimensional solid of atoms interacting through a variety of empirical potentials. These workers found that the ratio $\gamma_{us}^{(r)}/\mu b$ provides a useful means for characterizing the D–B behaviour, with the value 0·015 separating the two regimes, and ductile behaviour correspondings to smaller values of the ratio. From the results of the present study, we find that

$$\frac{\gamma_{us}^{(r)}}{\mu b} = 0{\cdot}0287 \tag{6}$$

when we use the value of μ calculated at the theoretical lattice constant of 3·95 Å. Our value for the ratio that characterizes D–B behaviour is larger than the criterion of Zhou *et al.* (1993, 1994) by a factor of almost two, again implying brittle behaviour for aluminium within this theoretical model.

One may question the ability of the present calculations to obtain accurate estimates of the fundamental quantities entering the D–B criteria. In defence of the accuracy of the present calculations (putting aside the comparison of theoretical results to available experimental numbers discussed in § 2), we invoke the following argument. Suppose that experimental numbers were used exclusively for the values of key quantities. A strict lower bound for the value of γ_{us} is the value of γ_{isf}, since the unstable stacking energy cannot be lower than the energy of the intrinsic stacking fault. Using the value of γ_{isf} as an approximation to γ_{us} and the experimental values for $\mu = 26{\cdot}5$ GPa, and $b = a_0/6^{1/2}$, $a_0 = 4{\cdot}05$ Å, one would obtain a ratio of $\gamma_{us}/\mu b$ in the range 0·025–0·064 (from the experimental values for γ_{isf} which range from 0·11 to 0·28 J m^{-2}). This is a lower bound (since γ_{isf} is a lower bound for γ_{us}) and is still much higher than the value of 0·015 proposed by Zhou *et al.* (1993, 1994) as separating brittle from ductile behaviour. In fact, the lowest value of this estimate is reasonably close to the result obtained from our first-principles calculations. This argument leads us to suggest that the surprising result obtained here, namely that aluminium is predicted to be brittle, is not due to limitations of the first-principles calculations.

We also wish to point out that surface energy terms associated with surface creation during dislocation emission and lattice trapping were not taken into account in the Peierls-type analysis discussed above. Both of these effects would tend to *increase* the value of the ratio $G_d/2\gamma_s$ relative to what has been reported here (for example Xu *et al.* (1995) and Juan, Sun and Kaxiras (1996)), tilting the balance towards more brittle behaviour. On the other hand, the atomistic simulations of Zhou *et al.* (1993, 1994), which do take these effects into account, nevertheless provide a picture consistent with the Peierls analysis.

These results pose an interesting puzzle. To our knowledge, there is no experimental indication of brittle behaviour in aluminium at finite temperatures. The resolution of the puzzle may be provided by three different possibilities.

(*a*) The theoretical framework invoked to discuss D–B behaviour applies to the *intrinsic* behaviour of a pure material; the behaviour of a material with a high density of pre-existing dislocations is not captured by this framework. Thus aluminium may be ductile owing to motion of pre-existing dislocations. Beltz, Rice, Shih and Xia (1996) recently addressed the issue of crack growth in the presence of a large number of pre-existing dislocations. Their analysis could provide important insight into the problem discussed here.

(*b*) Since, strictly speaking, the theoretical analysis presented above applies to zero temperature, aluminium may indeed be brittle at zero temperature and its ductility is due to thermally activated dislocation emission. Rice and Beltz (1994) have extended the Peierls framework to study thermally activated dislocation emission in certain cases.

(*c*) Finally, it is possible that significant improvements are required in order to provide quantitative theories that can predict the intrinsic D–B behaviour of a pure material. For example, the recent results of Xu *et al.* (1996, 1997) point to exciting new directions toward developing quantitative theories of the D–B transition that include more realistic representation of dislocation nucleation processes near a crack tip.

Acknowledgements

We wish to thank J. R. Rice for useful discussions and Vasily Bulatov for careful reading of the manuscript and helpful suggestions. This work was supported by the Office of Naval Research under Contract No. N00014-92-J-1960. The calculations were performed at the Pittsburgh Supercomputer Center.

References

Argon, A. S., Xu, G., and Ortiz, M., 1996, *Fracture—Instability, Dynamics, Scaling and Ductile/Brittle Behavior*, Materials Research Society Symposium Proceedings, Vol. 409, edited by R. Selinger, J. Mecholksy, A. Carlsson and E. Fuller, (Pittsburgh, Pennsylvania: Materials Research Society), p. 29.

Bachelet, G. B., Hamann, D. R., and Schlüter, M., 1982, *Phys. Rev.* B, **26**, 4199.

Beltz, G. E., and Rice, J. R., 1992, *Acta Metall.*, **40**, S321.

Beltz, G. E., Rice, J. R., Shih, C. F., and Xia, L., 1996, *Acta mater.*, **44**, 3943.

Denteneer, P. J. H., and Soler, J. M., 1991a, *J. Phys: condens. matter*, **3**, 877; 1991b, *Solid St. Commun.*, **78**, 857.

Cheung, K. S., 1990, PhD Thesis, Department of Nuclear Engineering, Massachusetts Institute of Technology, Cambridge, Massachusetts.

Ferrante, J., and Smith, J. R., 1979, *Phys. Rev.* B, **19**, 3991.

Griffith, A. A., 1920, *Phil. Trans. R. Soc.* A, **184**, 181.

Hirth, J. P., and Lothe, J., 1982, *Theory of Dislocations*, second edition (New York: Wiley).

Hohenberg, P., and Kohn, W., 1964, *Phys. Rev.*, **136**, B864.

Juan, Y. M., Sun, Y., and Kaxiras, E., 1996, *Phil. Mag. Lett.*, **73**, 233.

Kaxiras, E., and Duesbery, M. S., 1993, *Phys. Rev. Lett.*, **70**, 3752.

Kohn, W., and Sham, L., 1965, *Phys. Rev.*, **140**, A1133.

Mehl, M. J., and Boyer, L. L., 1991, *Phys. Rev.* B, **43**, 9498.

Mills, M. J., and Sadelmann, P., 1989, *Phil. Mag.* A. **60**, 355.

Monkhorst, H. J., and Pack, J. D., 1976, *Phys. Rev.* B, **13**, 5188.

Paxton, A. T., Gumbsch, P., and Methfessel, M., 1991, *Phil. Mag. Lett.*, **63**, 267.

Pearson, W. B., 1958, *A Handbook of Lattice Spacings and Structures of Metals and Alloys* (Oxford: Pergamon).

Peierls, B., 1940, *Proc. phys. Soc.*, **52**, 34.

Perdew, J., and Zunger, A., 1981, *Phys. Rev.* B, **23**, 5048.

Rice, J. R., 1992, *J. Mech. Phys. Solids*, **40**, 239.

Rice, J. R., and Beltz, G. E., 1994, *J. Mech. Phys. Solids*, **42**, 333.

Rice, J. R., Beltz, G. E., and Sun, Y., 1992, *Topics in Fracture and Fatigue*, edited by A. S. Argon (Berlin: Springer), p. 1.

Rice, J. R., and Thomson, R., 1974, *Phil. Mag.*, **29**, 73.

Rose, J. H., Smith, J. R., Guinea, F., and Ferrante, J., 1984, *Phys. Rev.* B, **29**, 2963.

Sun, Y., and Beltz, G. E., 1995, *J. Mech. Phys. Solids*, **42**, 1905.

Sun, Y., Beltz, G. E., and Rice, J. R., 1993, *Mater. Sci. Engng*, **A170**, 67.

Sun, Y., Rice, J. R., and Truskinovsky, L., 1991, *High Temperature Ordered Intermetallic Alloys*, Materials Research Society Symposium Proceedings, Vol. 213, edited by L. A. Johnson, D. T. Pope and J. O. Stiegler (Pittsburgh, Pennsylvania: Materials Research Society), p. 243.

Wright, A., Daw, M. S., and Fong, C. Y., 1992, *Phil. Mag.* A, **66**, 387.

Xu, G., Argon, A. S., and Ortiz, M., 1995, *Phil. Mag.* A, **72**, 415; 1996, to be published; 1997, *Phil. Mag.* A, **75**, 341.

Zhou, S. J., Carlsson, A. E., and Thomson, R., 1993, *Phys. Rev.* B, **47**, 7710; 1994, *Phys. Rev. Lett.*, **72**, 852.